Probing the Heme Axial Ligation in the CO-Sensing CooA Protein with Magnetic Circular Dichroism Spectroscopy†

Ish K. Dhawan,‡ Daniel Shelver,§ Marc V. Thorsteinsson,§ Gary P. Roberts,§ and Michael K. Johnson*,‡

Department of Chemistry and Center for Metalloenzyme Studies, University of Georgia, Athens, Georgia 30602, and Department of Bacteriology, University of Wisconsin−Madison, Madison, Wisconsin 53706

Received June 8, 1999; Revised Manuscript Received July 29, 1999

ABSTRACT: The combination of UV/visible/near-IR variable-temperature magnetic circular dichroism (VTMCD) and EPR spectroscopies has been used to investigate the spin states and axial ligation of the heme group in oxidized, reduced, and CO-bound reduced forms of the *Rhodospirillum rubrum* CO oxidation transcriptional activator protein (CooA) and its H77Y and C75S variants. The energy of the porphyrin-(π)-to-Fe(III) charge-transfer band (8930 cm^{-1}) and the presence of cysteinate S-to-Fe(III) charge-transfer bands between 600 and 700 nm confirm cysteinate axial ligation to the low-spin Fe(III) hemes in oxidized wild-type and H77Y CooA. In contrast, the major component in the oxidized C75S variant is shown to be a low-spin Fe(III) heme with bis-histidine or histidine/amine axial ligation on the basis of the energy of the porphyrin(π)-to-Fe(III) charge-transfer band (6240 cm^{-1}) and the anisotropy of the EPR signal, $g = 3.23, \sim 2.06, \sim 1.14$. These results confirm Cys75 as the cysteinyl axial ligand in oxidized CooA, indicate that it is replaced as an axial ligand by a histidine in the C75S variant, and reveal the presence of a hitherto unidentified histidine or neutral nitrogen ligand trans to Cys75 in wild-type CooA. Evidence for a Cys75-to-His77 axial ligand switch on reduction of CooA comes from VTMCD studies of the reduced proteins. The VTMCD spectra of reduced wild-type and C75S CooA are dominated by bands characteristic of bis-histidine low-spin Fe(II) hemes, whereas the reduced H77Y variant is predominantly high-spin with MCD characteristics typical of a five-coordinate, histidine-ligated ferrous heme. VTMCD studies show that the CO-bound reduced forms of wild-type, H77Y, and C75S contain low-spin Fe(II) hemes and that the Fe−CO bonds can be photolytically cleaved at temperatures <50 K. Strong evidence that CO binding to the heme group in reduced CooA occurs with displacement of His77 comes from the VTMCD spectra of the low-temperature photoproducts of CO-bound reduced forms of wild-type, H77Y, and C75S CooA. The spectra are almost identical to each other and closely correspond to those of the low-temperature photoproducts of well characterized CO-bound ferrous hemes with His/CO axial ligation.

In addition to their well-established roles in electron transfer, oxygen transport, and small molecule binding and activation, heme groups are known to act as sensors for NO in soluble guanylyl cyclase in order to regulate enzyme activity (*1*−*3*) and for O_2 in the rhizobial FixL protein in order to regulate gene expression (*4*−*6*). More recently, evidence has emerged for a heme-containing CO-sensing transcription factor, termed the CO oxidation activator (CooA),[1] in the photosynthetic bacterium *Rhodospirillum rubrum* (*7, 8*). CooA is a dimeric protein containing two heme groups which bind CO in the reduced form (*7*−*9*), thereby permitting CooA to activate two operons that encode a CO-oxidizing system (*10, 11*). By analogy with the homologous CRP family of proteins (*9*), the ability of CooA to bind DNA in a site-specific manner is believed to result from a conformational change that is induced by CO binding at the reduced heme groups (*12, 13*). Hence, determining the axial ligation of the heme groups in CooA and the changes induced by CO binding is central to any understanding of the CO-sensing mechanism.

Information concerning the axial ligation of the *b*-type hemes in CooA has come from the combination of spectroscopic and mutagenesis results (*8, 13*−*17*). Absorption and EPR studies of oxidized CooA indicate a six-coordinate low-spin ($S = 1/2$) ferric heme with cysteinate as one of the axial ligands (*14*). Subsequent mutagenesis results identified Cys75 as the axial cysteinyl ligand (*13, 15*), but the nature of the other axial ligand has remained elusive. Both the absorption and resonance Raman spectra of the functional reduced form of CooA are consistent with a six-coordinate low-spin ($S = 0$) ferrous heme (*13, 15*−*17*). However, absorption spectra coupled with mutagenesis studies involving the C75A and C75S variants have provided strong evidence that Cys75 is no longer an axial ligand in the reduced protein (*13, 15*).

† Supported by grants from the National Institutes of Health (GM 53228 to G.P.R. and GM 51962 to M.K.J.).

* To whom correspondence should be addressed at the Department of Chemistry, University of Georgia, Athens, GA 30602. Telephone: 706-542-9378; FAX: 706-542-2353; E-mail: johnson@sunchem.chem.uga.edu.

‡ University of Georgia.

§ University of Wisconsin−Madison.

[1] Abbreviations: CooA, CO oxidation activator; CRP, cAMP receptor protein; VTMCD, variable-temperature magnetic circular dichroism; DTT, dithiothreitol; iNOS, inducible nitric oxide synthase; MOPS, 3-(*N*-morpholino)propanesulfonic acid; EPPS, *N*-(2-hydroxyethyl)piperazine-*N*′-(3-propanesulfonic acid); CHES, 2-(*N*-cyclohexylamino)ethanesulfonic acid; WT, wild-type.

10.1021/bi991303c CCC: $18.00
Published on Web 09/11/1999

Rather, spectroscopic and functional studies of the H77Y and H77A variants (*13, 15*) indicate that the imidazole side chain of His77, or more likely the imidazolate formed by proton transfer to Cys75 (*13, 17*), is recruited as one of the axial ligands to the ferrous heme. The nature of the sixth ligand to the ferrous heme as well as the identity of the ligand that is displaced by CO binding remains undetermined.

To clarify the identity of the axial ligands and the spin states of the heme groups in wild-type (WT), H77Y, and C75S CooA, in the ferric, ferrous, and ferrous-CO forms, we have used variable-temperature magnetic circular dichroism (VTMCD) spectroscopy, in conjunction with parallel EPR studies. MCD has emerged as a powerful technique for studying hemoproteins due to its capability to distinguish hemes with similar absorption spectra and its potential to identify the nature and number of axial ligands through comparison with structurally characterized heme proteins and well-defined model complexes (*18, 19*). The ability of VTMCD to cleanly discriminate between diamagnetic low-spin ($S = 0$) and paramagnetic high-spin ($S = 2$) ferrous hemes (*19*) and to address the axial ligation of low-spin ferric hemes via the energy of the porphyrin(π)-to-Fe(III) charge-transfer bands (*20, 21*) is particularly useful with respect to ongoing attempts to characterize the novel heme center in CooA. In addition to supporting the proposed redox-controlled ligand exchange (*13, 15, 17*), the results provide insight into the nature of the sixth ligand in oxidized and reduced CooA and the ligand replaced by CO in reduced CooA.

MATERIALS AND METHODS

CooA Samples. Heterologously expressed WT CooA and the C75S and H77Y variants were prepared as previously described (*13*). The C75S CooA samples used in this work were isolated anaerobically in the presence of 1 mM sodium dithionite, and in the absence of DTT. Oxidized samples of the C75S variant were obtained by addition of a slight excess ferricyanide which was subsequently removed via anaerobic gel filtration. WT and H77Y CooA were prepared aerobically in the oxidized state in 25 mM MOPS buffer, pH 7.4, with 0.1 M NaCl, and were reduced under anaerobic conditions by the addition of 1 mM sodium dithionite. CO-bound forms of the reduced samples were obtained by incubation under 1 atm of CO at room temperature for 15 min. Studies of the H77Y mutant as a function of pH were carried out on samples exchanged into 25 mM EPPS buffer at pH 8.5 or 25 mM CHES buffer at pH 10.0.

Spectroscopic Methods. Absorption spectra were recorded on a Shimadzu UV301PC spectrophotometer. Variable-temperature and variable-field MCD measurements were recorded on samples containing 55% (v/v) glycerol or glycerol-d_3 using a Jasco J-715 (180−1000 nm) or a Jasco J-730 (700−2000 nm) spectropolarimeter mated to an Oxford Instruments Spectromag 4000 (0−7 T) split-coil superconducting magnet. The experimental protocols for measuring MCD spectra of oxygen-sensitive samples over the temperature range 1.5−300 K with magnetic fields up to 7 T have been described elsewhere (*22, 23*). X-band (~9.6 GHz) EPR spectra were recorded on a Bruker ESP-300E EPR spectrometer with a dual-mode ER-4116 cavity and equipped with an Oxford Instruments ESR-9 flow cryostat (4.2−300 K). Frequencies were measured with a Hewlett-Packard 5350B frequency counter, and the field was calibrated with a Bruker ER 035M gaussmeter. Spin quantitations were carried out using a 1 mM CuEDTA standard under nonsaturating conditions according to the published procedures (*24*).

RESULTS AND DISCUSSION

Oxidized Wild-Type and Mutant Forms of CooA

UV/visible/near-IR VTMCD spectra for the as-isolated (oxidized) forms of WT, H77Y, and C75S CooA are shown in Figure 1 and the corresponding X-band EPR spectra of these samples measured at 22 K are shown in Figure 2. Identical EPR spectra were obtained for samples in the absence of glycerol, and the spectra are in good agreement with previously published EPR data for WT and H77Y CooA, and C75S CooA samples isolated without DTT in the final purification step (*13, 14*). The VTMCD spectra are all characteristic of low-spin Fe(III) hemes (*19*), and MCD magnetization studies (not shown) confirm an $S = 1/2$ ground state.

Cys75 Is a Heme Axial Ligand in Oxidized WT CooA. Mutagenesis studies monitored by UV/visible absorption and EPR have provided strong evidence that Cys75 is one of the heme axial ligands in oxidized WT CooA (*13, 15)*. This conclusion is further substantiated by the VTMCD studies reported herein. Although the VTMCD spectra of low-spin Fe(III) hemes in the region of the α, β, and Soret $\pi \rightarrow \pi^*$ transitions are not particularly sensitive to the nature of the axial ligands, the near-identical VTMCD spectra of the WT and H77Y samples serve to demonstrate that this mutation does not alter the heme axial ligation or excited-state electronic structure. In contrast, the Soret MCD for the C75S variant (crossover at 411 nm) is blue shifted by 8 nm compared to WT and H77Y CooA (crossover at 419 nm), and there are significant differences in the α, β region. Direct evidence that the differences in the UV−visible VTMCD spectra of oxidized WT and C75S CooA arise from a change in axial ligation of the heme Fe in the C75S variant comes from near-IR VTMCD spectra in both the S-to-Fe(III) and porphyrin(π)-to-Fe(III) charge-transfer regions.

In the S-to-Fe(III) charge-transfer region, both WT and H77Y have positive and negative temperature-dependent bands (*C*-terms) centered at 636 and 676 nm, respectively, that are not present in the C75S variant (Figure 1). Similar bands have been observed in native and imidazole-bound forms of P450 (positive bands at 624 and 628 nm, respectively, and negative bands at 665 and 647 nm, respectively) and have been attributed to thiolate S-to-Fe(III) [p_y-d(t_{2g}) hole and p_z-d(t_{2g}) hole] charge-transfer transitions (*25*). Hence, the loss of these transitions in the C75S variant shows that Cys75 is an axial ligand to the low-spin Fe(III) heme in WT and H77Y CooA.

The porphyrin(π)-to-Fe(III) charge-transfer bands of low-spin Fe(III) hemes occur in the 800−2400 nm region, and their energies are very sensitive to the nature of the heme axial ligands (*19*−*21*). These bands are difficult to observe in the electronic absorption spectrum due to the overlap with O−H, C−H, and N−H vibrational overtones from water or protein, but are readily observed as two positive *C*-terms in the near-IR VTMCD spectrum. The lower energy component

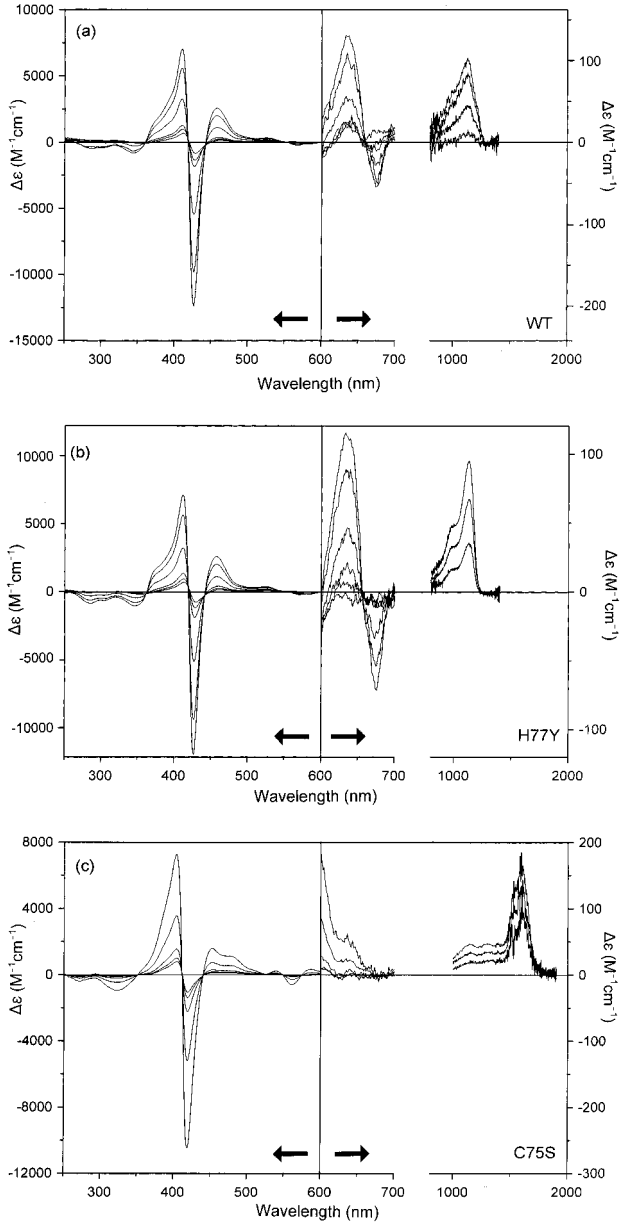

FIGURE 1: VTMCD spectra of as-isolated WT, H77Y, and C75S CooA. The samples were in 25 mM MOPS with 0.1 M NaCl at pH 7.4 with 55% (v/v) glycerol-d_3, and in all cases the intensities of all MCD bands increase with decreasing temperature. (a) WT CooA, 45 μM in heme. UV−vis MCD spectra (200−700 nm) were recorded at temperatures of 1.92, 4.22, 9.9, 32, 45, and 77 K, with a magnetic field of 6.0 T. The NIR MCD spectra (800−1500 nm) were recorded at temperatures of 1.91, 4.22, 9.9, and 32 K, with a magnetic field of 6.0 T. (b) H77Y CooA, 80 μM in heme. In the UV−vis region (200−700 nm), the spectra were recorded at temperatures of 1.93, 4.22, 10.2, 30, 49, and 81 K, with a magnetic field of 6.0 T. The sample concentration was 161 μM in heme for the NIR region (800−1500 nm), and the spectra were recorded at temperatures of 1.95, 4.22, and 10.2 K with a magnetic field of 4.5 T. (c) C75S CooA, 118 μM in heme. In the UV−vis region (200−700 nm), the spectra were recorded at temperatures of 4.22, 10.9, 29, 50, and 66 K with a magnetic field of 4.5 T. The sample concentration was 118 μM in heme for the NIR region (800−1500 nm), and the spectra were recorded at temperatures of 1.96, 4.22, and 10.2 K with a magnetic field of 4.5 T.

is invariably more intense and serves as a direct measure of the a_{1u}-d(t_{2g}) hole porphyrin(π)-to-Fe(III) charge-transfer energy, E_{CT} (Table 1 and Figure 1). Thomson and co-workers have developed the relationship between ground state g-value

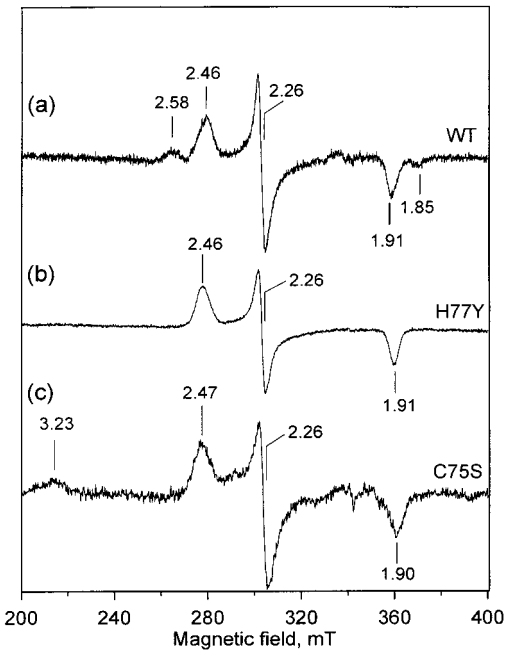

FIGURE 2: X-band EPR spectra of the VTMCD samples of as-isolated WT, H77Y, and C75S CooA. (a) WT CooA; sample identical to that used in Figure 1(a). (b) H77Y CooA; sample identical to that used in Figure 1(b) for UV−vis VTMCD. (c) C75S CooA; sample identical to that used in Figure 1(c) for UV−vis VTMCD. EPR conditions: temperature, 22 K; microwave power, 2 mW; modulation amplitude, 0.8 mT; microwave frequency, 9.59 GHz.

anisotropy as determined by EPR and E_{CT}, as measured by near-IR MCD studies, and this has led to ranges being established for E_{CT} for different pairs of axial ligands (*19*−*21*, *25*). Hence, the value of E_{CT} for WT and H77Y CooA (8930 cm^{-1}) is indicative of low-spin Fe(III) hemes with an axial thiolate ligand (E_{CT} in the range 7800−9400 cm^{-1}; see Table 1). In contrast, the porphyrin(π)-to-Fe(III) charge-transfer bands for C75S CooA occur at much lower energies, $E_{CT} = 6240$ cm^{-1}, well outside of the range associated with an axial thiolate ligand, and in accord with axial ligation by Cys75 in WT and H77Y CooA.

Previous EPR studies of WT CooA revealed a minor component, $g = 2.58, 2.26, 1.85$ (compared to $g = 2.46, 2.26, 1.91$ for the major component), corresponding to ∼15% of the heme at pH 7.4 (*13*, *14*). This species was present in the samples used for near-IR VTMCD and is apparent by a low-energy shoulder at ∼1200 nm on the porphyrin-to-Fe(III) charge-transfer bands of WT CooA [Figure 1(a)], indicating $E_{CT} \sim 8300$ cm^{-1}. The presence of this shoulder in WT CooA is best illustrated by comparison with the near-IR VTMCD spectrum of H77Y CooA [Figure 1(b)], which has a homogeneous low-spin Fe(III) heme [$g = 2.46, 2.26, 1.91$ (Figure 2)]. As for the major component, the EPR and near-IR MCD data for this minor component can only be interpreted in terms of an axial cysteinate ligand.

Nature of the Heme Ligand trans to Cys75 in Oxidized WT CooA. While the near-IR VTMCD and EPR data are unambiguous in assigning a cysteinate as one of the axial heme Fe ligands in both the oxidized forms of WT and H77Y CooA, the nature of the other axial ligand is less well-defined. In large part, this is due to the paucity of near-IR MCD data for cysteinate-ligated, structurally characterized low-spin Fe(III) hemes. Near-IR VTMCD data are currently only

Table 1: EPR *g*-Values and Energies of Near-IR Charge Transfer Bands of Low-Spin Fe(III) Species in WT and Mutant Forms of CooA and Related Proteins[a]

protein	axial ligands	g_z	g_y	g_x	E_{CT} (cm^{-1})	ref
WT CooA (major)	Cys/His or amine[b]	2.46	2.26	1.91	8930	this work
WT CooA (minor)	Cys/His or amine[b]	2.58	2.26	1.85	~8300	this work
CooA + Im	Cys/Im	2.52	2.27	1.85	na	this work
H77Y CooA	Cys/His or amine[b]	2.46	2.26	1.91	8930	this work
C75S CooA (major)	His/His or amine[b]	3.23	2.06	1.14	6240	this work
C75S CooA (minor)	RS^-/His or amine[b]	2.47	2.26	1.90	8930	this work
P450 BM-3	Cys/H_2O	2.42	2.26	1.92	9400	*25*
P450 BM-3 + Im	Cys/Im	2.61	2.25	1.83	8470	*25*
$P450_{CAM}$	Cys/H_2O	2.45	2.26	1.91	na	*26*
$P450_{CAM}$ + Im	Cys/Im	2.56	2.27	1.87	na	*26*
$P450_{CAM}$ + PIm	Cys/PIm	2.47	2.27	1.89	na	*26*
P420	Cys/His or amine[b]	2.45	2.27	1.91	na	*27*
iNOS	Cys/H_2O	2.42	2.30	1.91	8330	*c*
iNOS + Im	Cys/Im	2.54	2.31	1.85	7810	*c*
M80C cyt *c*	Cys/His	2.56	2.27	1.85	na	*28*
H450 (major, pH 8.0)	Cys/His or amine[b]	2.42	2.28	1.91	na	*29*
H450 (major, pH 6.0)	Cys/His or amine[b]	2.51	2.33	1.87	na	*29*
C450 (pH 6.0)	Cys/H_2O	2.63	2.26	1.83	na	*30*
C450 + PIm	Cys/PIm	2.51	2.28	1.87	na	*31*
C420	Cys/His or amine[b]	2.48	2.27	1.89	na	*32*

[a] g_z, g_y, and g_x refer to the maximum, crossover, and minimum of the resonance, respectively; na, not available; Im, imidazole; PIm, *N*-phenylimidazole; P450 BM-3, fatty acid mono-oxygenating P450 from *Bacillus megaterium.* [b] Axial ligand assignment based on or by analogy with this work. Amine refers to lysine, arginine, or the N-terminus of the polypeptide. [c] Garton, S. D., Rafferty, S., Malech, H. L., and Johnson, M. K., manuscript in preparation.

available for native and imidazole-bound forms of P450 and the inducible nitric oxide synthase (iNOS) (see Table 1). These data provide an initial frame of reference for assessing the CooA results, but the data set is too limited to provide definitive evidence as to the nature of the sixth ligand. Crystallographic and spectroscopic studies indicate Cys/H_2O axial ligation for the low-spin Fe(III) forms of the native P450 and iNOS (*33*, *34*), and these enzymes have E_{CT} = 9400 and 8330 cm^{-1}, respectively. Hence, the major component of WT CooA and H77Y CooA, which has E_{CT} = 8930 cm^{-1}, lies in the range of energies established for Cys/H_2O axial heme ligation. The imidazole-bound forms of P450 and iNOS have E_{CT} = 8470 and 7810 cm^{-1}, respectively, both lower than the major component of WT CooA and H77Y CooA, but similar to that of the minor component in WT CooA (E_{CT} ~ 8300 cm^{-1}). This observation, together with the increase in *g*-value anisotropy that accompanies imidazole binding in P450 and iNOS (Table 1), and the EPR properties of the Cys/His-ligated low-spin Fe(III) heme in Met80Cys cytochrome *c* (g = 2.56, 2.27, 1.85; see Table 1), raises the possibility that the minor species has Cys/His axial ligation. Hence, the EPR and VTMCD data for WT oxidized CooA can be satisfactorily interpreted in terms of the major and minor low-spin Fe(III) heme components having Cys/H_2O and Cys/His axial ligation, respectively. However, as discussed below, such a model is not consistent with the exogenous ligand binding studies and VTMCD data for oxidized C75S CooA.

By analogy with P450 and iNOS, an axial H_2O might be expected to be readily replaceable by exogenous ligands such as imidazole, resulting in a derivative with similar properties to the minor component in WT CooA. However, ligand binding experiments with imidazole show that the heme center in CooA is remarkably resistant to exogenous ligand binding. No significant perturbation of the absorption or EPR properties was apparent with up to a 100-fold excess of imidazole. Room-temperature incubation with 200-fold to

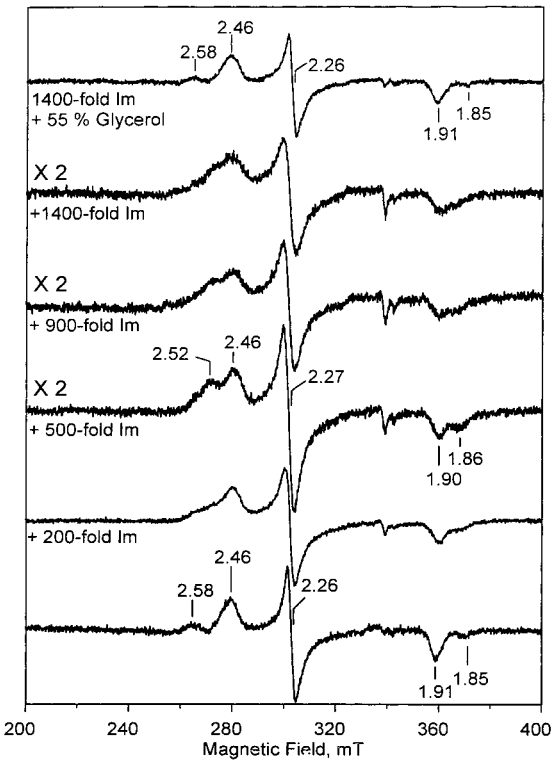

FIGURE 3: Effect of imidazole on the X-band EPR spectra of as-isolated CooA. The sample, 60 μM in heme, was in 25 mM MOPS with 0.1 M NaCl at pH 7.4. EPR conditions: temperature, 22 K; microwave power, 2 mW; modulation amplitude, 0.6 mT; microwave frequency, 9.59 GHz.

1400-fold stoichiometric excesses of imidazole does result in the emergence of a new EPR signal with g = 2.52, 2.26, 1.86 (Figure 3), that is readily interpreted as a low-spin Fe(III) heme with Cys/imidazole axial ligation (Table 1). However, the EPR spectrum reverts to that of the WT upon addition of 55% (v/v) glycerol, thereby preventing investigation with VTMCD. Spectral simulations (not shown) indicate

that this resonance maximally accounts for 30% of the total low-spin Fe(III) heme resonance and that it derives from both the major and minor components, since both are present in the same ratio in imidazole-bound samples. While it appears to be possible to partially replace the sixth ligand with high concentrations of imidazole, it seems very unlikely that the observed heterogeneity in the low-spin Fe(III) heme results from differences in the sixth axial ligand with one form corresponding to a H_2O-bound species.

Although the loss of the minor component in the H77Y variant could be construed as implicating His77 as the histidine axial ligand responsible for the minor component, the single-residue spacing between Cys75 and His77 rules out the possibility that both can act as trans axial ligands to the same low-spin Fe(III) heme. Rather, as pointed out previously (*13*), the heterogeneity in the low-spin Fe(III) heme of WT CooA is more likely to be a consequence of an interaction between His77 and Cys75. Both resonance Raman and absorption studies of WT and H77Y CooA are consistent with a redox-dependent axial ligand switch with His77 replacing Cys75 on reduction (*13, 15, 17*), and this is further supported by the VTMCD data on the reduced samples presented below. Moreover, the resonance Raman data for reduced CooA suggest that this occurs via protonation of Cys75 by the imidazole side chain of His77 and binding of the histidinate form of His77 (*17*). Hence, the observed pH dependence of the EPR spectrum of WT CooA, i.e., minor: major component ratios of 5:95 at pH 8.5, 15:85 at pH 7.4, and 25:75 at pH 6.5 (*13*), has been rationalized based on the minor species corresponding to a coordinated cystiene thiol formed via proton transfer from His77. However, to our knowledge there are no well-documented examples of thiol-ligated hemes, and a thiol might be expected to approximate more to a methionine than a cysteinate ligand. A thiolate to thiol change in axial ligation would therefore be expected to result in a 2000−3000 cm^{-1} decrease in E_{CT} (*19, 25*) and a concomitant large increase in *g*-value anisotropy. While it is difficult to reconcile the small increase in the *g*-value anisotropy and small decrease in E_{CT} for the minor species (compared to the major species), with a coordinated thiol, such behavior could result from a hydrogen-bonding interaction between Cys75 and His77. Hence, two different conformations in frozen solution, one with and one without this hydrogen-bonding interaction, are currently our best interpretation for the observed heterogeneity in the low-spin Fe(III) form of WT CooA.

More direct evidence for histidine or some other neutral nitrogen ligand as the sixth ligand to the low-spin Fe(III) hemes in WT and H77Y CooA comes from the near-IR VTMCD and EPR studies of C75S CooA samples purified anaerobically in the absence of DTT and oxidized with ferricyanide. In addition to the loss of the cysteinate S-to-Fe(III) charge-transfer transitions in the 600−700 nm region of the VTMCD spectrum, the porphyrin(π)-to-Fe(III) charge-transfer band is red-shifted to 1600 nm (E_{CT} = 6240 cm^{-1}) [Figure 1(c) and Table 1]. This band position is in the middle of the range established for bis-histidine (or histidine/imidazole) ligated low-spin Fe(III) hemes, 1500−1660 nm (E_{CT} = 6020−6670 cm^{-1}), and just outside the range established for histidine/lysine, histidine/N-terminal amine, or histidine/amine, 1480−1550 nm (E_{CT} = 6450−6760 cm^{-1}) (*19, 20, 35*). Although the energy of the porphyrin(π)-to-Fe(III) charge-transfer band favors bis-histidine axial ligation, histidine/amine axial ligation cannot be ruled out at this stage since the above-mentioned range is based on a handful of samples.

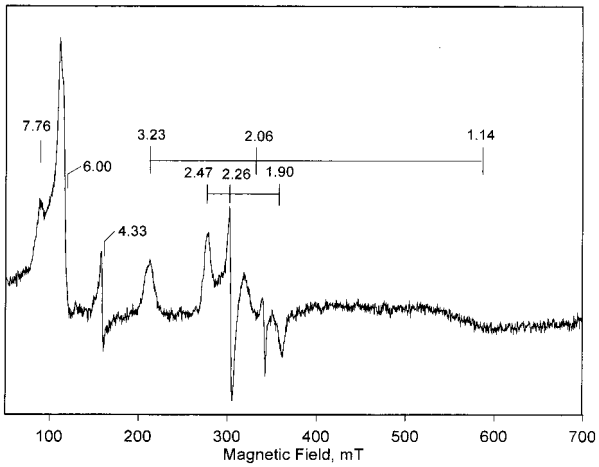

FIGURE 4: X-band EPR spectrum of as-isolated C75S CooA. The sample is the same as that used in Figure 2(c). EPR conditions: temperature, 10 K; microwave power, 5 mW; modulation amplitude, 0.6 mT; microwave frequency, 9.59 GHz.

The VTMCD evidence for a bis-histidine or histidine/amine ligated low-spin Fe(III) heme in C75S CooA purified in the absence of DTT prompted a detailed EPR study over the temperature range 4.2−30 K with microwave powers between 0.01 and 100 mW, since such a species would be expected to exhibit a more anisotropic EPR signal than a thiolate-coordinated low-spin Fe(III) heme. In accord with the published data for samples of the C75S variant isolated without DTT in the final purification step (*13*), EPR spectra recorded at 22 K exhibited a $g = 6$ resonance indicative of a high-spin Fe(III) heme component and a low-spin Fe(III) heme resonance, $g = 2.47, 2.26, 1.90$, almost indistinguishable from the major species in WT CooA (Figure 2). However, spin quantitations revealed that the "$g = 2.47$" low-spin resonance is a minor species accounting for only 0.1 spin/molecule. Closer inspection of the $S = 1/2$ region reveals an additional absorption-shaped feature at $g = 3.23$, that was present in the previously published data (*13*), but not commented on. A broader scan at 10 K shows that the $g = 3.23$ feature arises from a faster relaxing $S = 1/2$ species that is already significantly broadened at 22 K. Temperature dependence studies indicate that the other two components of this resonance are a broad derivative centered around $g = 2.06$ and a broad negative feature centered around $g = 1.14$ (Figure 4). In agreement with the near-IR MCD data, these *g*-values place this resonance into the category of low-spin Fe(III) hemes with bis-histidine or histidine/amine axial ligation on the basis of a plot of V/Δ and Δ/λ (*36*). Quantitation of this resonance versus the $g = 2.47, 2.26, 1.90$ resonance, using the procedure developed by Aasa and Vänngård (*24*) for quantifying resonances based on the integrated area of a well-resolved low-field ($g = 3.23$) component, indicates that this resonance accounts for 0.7 spin/molecule. Hence, this is the major heme species in the C75S variant with the remaining 20% attributed to the high-spin Fe(III) heme. The minor $g = 2.47, 2.26, 1.90$ component does exhibit a weak porphyrin-to-Fe(III) charge-transfer band at 1120 nm in the near-IR [Figure 1(c)]. Hence, it corre-

sponds to a thiolate-ligated low-spin Fe(III) heme, but the origin of the thiolate ligand is unclear at present, since the sample was purified in the strict absence of DTT. The propensity to bind thiolates at this site is demonstrated by the observation that addition of DTT to the C75S variant (data not shown) or purification of the C75S variant in the presence of DTT (*13*) results in loss of both the high-spin Fe(III) resonance and the "$g = 3.23$" low-spin Fe(III) resonance and the appearance of a new resonance, $g = 2.35$, 2.23, 1.93, that is attributed to a DTT-bound form.

In light of the evidence for reductive replacement of C75 by H77 as an axial heme ligand (see below and refs *13, 15, 17*), His77 is proposed to provide one of the axial ligands to the major low-spin Fe(III) heme component in the C75S variant. While it is possible that both axial ligands are perturbed via this mutation, the more likely rationalization is that a yet-to-be-identified histidine or amine residue provides the sixth ligand in WT, C75S, and H77Y CooA. We conclude that Cys/His or Cys/amine axial ligation for the low-spin Fe(III) heme in WT CooA provides the best rationalization for the absorption, resonance Raman, and EPR data (*14, 17*), is consistent with the near-IR VTMCD data presented herein, and accounts for the relative insensitivity to binding exogenous ligands such as imidazole. The possibility of a histidine or lysine ligand trans to Cys75 has been assessed via His-to-Cys (*13)* and His-to-Ala (*15*) mutations involving each of the four other histidine residues of CooA (at positions 28, 133, 146, and 200) and Lys-to-Ala mutations involving the lysines at positions 26, 30, and 101 (*15*). None of these mutations had a major effect on the electronic absorption spectra or on the ability of CooA to function as a CO sensor. However, in light of the possibility of a mutation-induced change in axial ligand and the relative insensitivity of the absorption spectra of the cysteinate-ligated low-spin Fe(III) heme in P450 to the nature of the trans ligand (*37*), it is not yet possible to rule out these histidines or lysines as axial ligands in WT CooA. In light of the VTMCD results, there is a pressing need to investigate the spectroscopic properties of these variants in more detail and to target other potential amine ligands such as arginines and the remaining lysines in future mutagenesis studies.

The present study also highlights the need for near-IR VTMCD studies of a wide range of cysteinate-ligated low-spin Fe(III) hemoproteins. A list of the relevant proteins and their EPR properties is presented in Table 1. Clearly, comparative near-IR MCD studies of WT and imidazole-bound forms of the structurally characterized cysteinate-ligated low-spin Fe(III) form of chloroperoxidase (C450), which has anomalous EPR compared to other cysteinate-ligated hemes, would be very informative. Likewise, there is an urgent need for near-IR VTMCD studies of the inactive low-spin Fe(III) forms of P450 and chloroperoxidase, termed P420 and C420, respectively, and of hemoprotein H450, which all have absorption and EPR properties very similar to those of WT and H77Y CooA. Unfortunately, the nature of the heme axial ligation in these proteins is still the subject of debate. For example, both coordination of a histidine trans to cysteine and weakening of the coordinated cysteine via protonation have been invoked to explain anomalous spectroscopic and exogenous ligand binding properties of P420 (*27, 38*) and C420 (*32*).

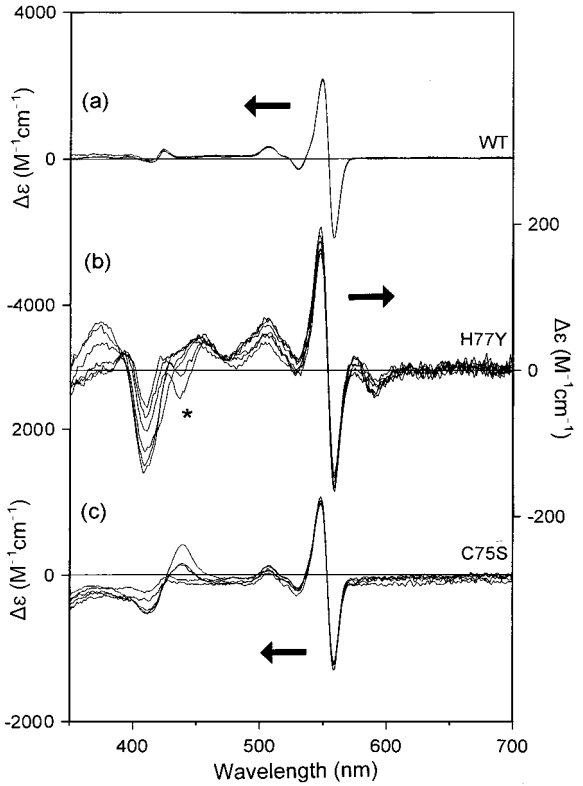

FIGURE 5: VTMCD spectra of dithionite-reduced WT, H77Y, and C75S CooA. (a) WT CooA. The sample was 41 μM in heme, and the buffering medium was as described in Figure 1, except for the anaerobic reduction with 2 mM sodium dithionite. The MCD spectra were recorded at temperatures of 1.95, 4.22, and 10.1 K with a magnetic field of 6.0 T. (b) H77Y CooA. The sample was 45 μM in heme, and the anaerobic buffering medium was 25 mM EPPS, pH 8.5, buffer with 55% (v/v) glycerol and 10 mM sodium dithionite. The MCD spectra were recorded at temperatures of 1.94, 4.22, 10.3, 28, 46, and 80 K with a magnetic field of 4.5 T. The MCD spectra contained features arising from unreduced, ferric H77Y CooA. These features have been subtracted from data shown, and the residual ferric CooA component that remains after subtraction is indicated with an asterisk. (c) C75S CooA. The sample was 32 μM in heme, and the buffering medium was as described in Figure 1 except for anaerobic reduction with 2 mM sodium dithionite. The MCD spectra were recorded at temperatures of 1.93, 4.22, 10.2, 28, and 45 K with a magnetic field of 6.0 T.

Reduced Wild-Type and Mutant Forms of CooA

VTMCD provides a valuable means of determining the spin state and assessing the axial ligation of ferrous hemes (*18, 19*). Spin state determination is straightforward, since paramagnetic ($S = 2$) high-spin Fe(II) forms exhibit temperature-dependent MCD spectra, whereas diamagnetic ($S = 0$) low-spin Fe(II) forms exhibit MCD spectra that are essentially temperature independent (except for effects due to narrowing of line widths at low temperatures). However, quantitative assessment of spin mixtures is difficult unless reliable MCD $\Delta\epsilon$ values are available for both the high-spin and low-spin forms.

Change of Axial Ligands on Reduction. VTMCD spectra for dithionite-reduced forms of WT, H77Y, and C75S CooA obtained with temperatures between 1.9 and 80 K are shown in Figure 5. The absence of temperature dependence for WT CooA shows that the heme is 100% low-spin Fe(II), in accord with the available absorption and resonance Raman data (*13*−*17*). Moreover, the observed spectrum with Soret- and

α-band *A*-terms centered at 420 and 554 nm, respectively, is indistinguishable from those well-characterized bis-histidine low-spin Fe(II) hemoproteins, e.g., *b*-type cytochromes (*39*), and very similar to those of P420 (*27*) and C420 (*32*). Thiolate-ligated low-spin Fe(II) hemes typically have Soret-band MCD centered at approximately 450 nm and α-band MCD centered between 540 and 550 nm. Hence, the VTMCD data support the proposals that the cysteine ligand is replaced by a histidine (or histidinate) on reduction (*13*, *15*, *17*), and that the trans ligand is another histidine or some other neutral nitrogen ligand.

Identification of the histidine that replaces Cys75 as an axial ligand on reduction is provided by VTMCD studies of reduced H77Y CooA. Complete reduction of this variant by dithionite has yet to be achieved for samples purified in this laboratory (*13*), and even minor amounts of low-spin Fe(III) hemes tend to dominate the MCD spectrum at low temperature. In this work, maximal reduction was achieved by anaerobic incubation with 10 mM dithionite in a pH 8.5 EPPS buffer at room temperature for 30 min. Even under these conditions, approximately 1% of the heme remained in the low-spin Fe(III) state as judged by the Soret band VTMCD intensity. The contribution from the unreduced species has been minimized in Figure 5(b), by subtracting the MCD spectrum of the as-isolated sample under identical conditions. In accord with resonance Raman studies (*17*), the presence of temperature-dependent and temperature-independent bands in the resultant VTMCD spectra indicates a mixture of high-spin and low-spin Fe(II) species in reduced H77Y CooA. If the low-spin Fe(II) form is identical to that found in WT, then the MCD intensity would suggest a 90:10 high-spin:low-spin ratio. However, this assumption is unlikely to be strictly valid, since the low-spin to high-spin transition on going from WT to H77Y is directly attributed to the loss of His77 as an axial ligand to the reduced heme. The high-spin Fe(II) component has temperature-dependent MCD bands throughout the 350−600 nm region [Figure 5(b)], and the form of the spectrum is similar to that of deoxymyoglobin (*19*, *40*, *41*), the archetypical mono-histidyl-ligated high-spin Fe(II) heme. [A positive band is expected at ∼430 nm, but this is obscured by the residual low-spin Fe(III) heme which has an intense positive band in this region (Figure 1(b).] Hence, the VTMCD data indicate that the H77Y substitution induces a low-spin to high-spin transition, in accord with the proposal that His77 is an axial ligand to the reduced WT CooA, and suggest that the resultant Fe(II) heme in the H77Y variant remains attached to the protein by axial ligation of a histidine or some other neutral nitrogen ligand.

The VTMCD spectrum of dithionite-reduced C75S CooA also reveals a mixture of high-spin and low-spin Fe(II) hemes [Figure 5(c)]. However, the relative intensities of the temperature-dependent and temperature-independent MCD bands suggest a much smaller high-spin component than in reduced H77Y CooA. Above 30 K, the temperature dependence is no longer apparent, and the resulting spectrum is identical to that of reduced WT CooA, further demonstrating that Cys75 is no longer a ligand to the low-spin Fe(II) heme in CooA. On the basis of the intensity of the pronounced α-band *A*-term centered at 554 nm, the heme in reduced C75S CooA is estimated to be ∼60% low spin. The partial low-spin to high-spin conversion in the C75S variant provides additional evidence for an interaction between His77 and Cys75 in the WT reduced protein.

CO Binding and Low-Temperature Photolysis. Determining which axial ligand to the low-spin Fe(II) heme in CooA is released on CO binding is clearly of fundamental importance in understanding the triggering mechanism of CO sensing. The recent resonance Raman studies of Spiro and co-workers favor displacement of His77 imidazolate by CO (*17*), since the Fe−CO and C−O stretching frequencies in the WT CO adduct are best interpreted in terms of a neutral trans ligand and a negative polarity in the CO binding pocket. However, the latter result is in conflict with resonance Raman studies of Uchida et al. (*16*), which suggested an apolar environment for CO in CO-bound reduced CooA and argued in favor of His77 being the ligand retained on CO binding. Hence, a major objective of the VTMCD studies of CO-bound forms of reduced WT, H77Y, and C75S CooA was to identify the ligand displaced by CO.

The reduced samples WT, H77Y, and C75S CooA all bound CO, and the electronic absorption spectra are characteristic of low-spin Fe(II) hemes (*13*). However, it proved difficult to characterize the MCD spectra of these adducts at liquid helium temperatures, since photolytic cleavage of the Fe−CO bond occurs progressively during the course of the measurements, yielding the intense temperature-dependent MCD spectra of high-spin, five-coordinate photoproduct. As the temperature is raised, the MCD intensity from the paramagnetic high-spin Fe(II) heme initially decreases, but conversion to the temperature-independent spectrum of a low-spin CO-bound ferrous form due to thermal recombination of CO starts to occur at around 50 K and is complete by 70 K (data not shown). Such photolysis behavior is not uncommon in CO-bound ferrous hemoproteins and has been extensively studied by VTMCD in hemoglobin, myoglobin, heme a_3 of cytochrome *c* oxidase (*42*), and in P450 (*43*).

To obtain homogeneous samples of the low-temperature photolysis products of the CO-bound forms of reduced WT, H77Y, and C75S CooA, samples were exposed to a 100 W Xe arc lamp at 4.2 K until there was no further increase in the MCD intensity (approximately 30 min) The resulting spectra obtained at 4.2 K are shown in Figure 6. Each is temperature-dependent, and magnetic-field-dependent studies carried out at 1.9, 4.2, and 10 K (not shown) are characteristic of an $S = 2$ ground state with positive zero-field splitting leaving the $M_s = 0$ level lowest in energy (*19*, *44*). The resultant spectra are very similar to each other and to those reported for the low-temperature photolysis products of the His/CO ligated low-spin Fe(II) hemes in hemoglobin, myoglobin, and heme a_3 of cytochrome *c* oxidase (*42*) and quite distinct from that reported for the low-temperature photolysis product of the Cys/CO ligated low-spin Fe(II) heme in P450 (*43*). This argues strongly in favor of the ligand trans to CO being the same in all three samples, which can only occur if the CO binding in WT and C75S CooA occurs with displacement of the His77 ligand. Moreover, it provides additional support for an indigenous unidentified histidine or amine ligand that remains coordinated in both redox states and is not displaced by CO.

The MCD spectra of the CO-bound low-spin Fe(II) hemes in WT, H77Y, and C75S CooA obtained at temperatures above 70 K are compared in Figure 7. For the H77Y and C75S samples, identical spectra, albeit with much lower

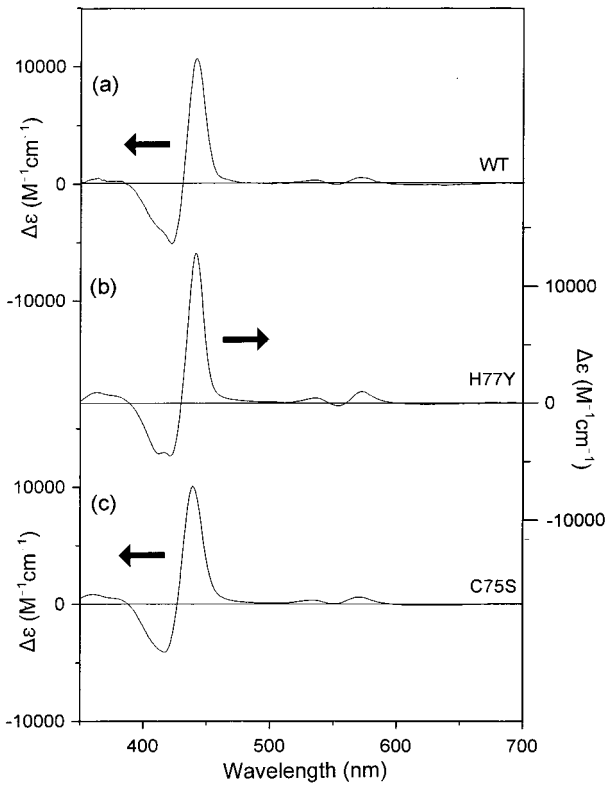

FIGURE 6: MCD spectra of the low-temperature photolysis products of the dithionite-reduced CO adducts of WT, H77Y, and C75S CooA at 4.22 K. The samples were photolyzed at 4.22 K for 0.5 h with a Xe arc lamp prior to data collection. (a) WT CooA. The sample is as described in Figure 4(a) except for incubation under CO atmosphere for 15 min at room temperature. The MCD spectrum was recorded with a magnetic field of 6.0 T. (b) H77Y CooA adduct. The sample was 127 μM in heme, and the buffering medium was as described in Figure 1 except for anaerobic addition of 2 mM sodium dithionite followed by incubation under CO atmosphere for 15 min at room temperature. The MCD spectrum was recorded with a magnetic field of 4.5 T. (c) C75S CooA. The sample was 87 μM in heme, and the buffering medium was as described in Figure 1 except for anaerobic addition of 2 mM sodium dithionite followed by incubation under CO atmosphere for 15 min at room temperature. The MCD spectrum was recorded with a magnetic field of 4.5 T.

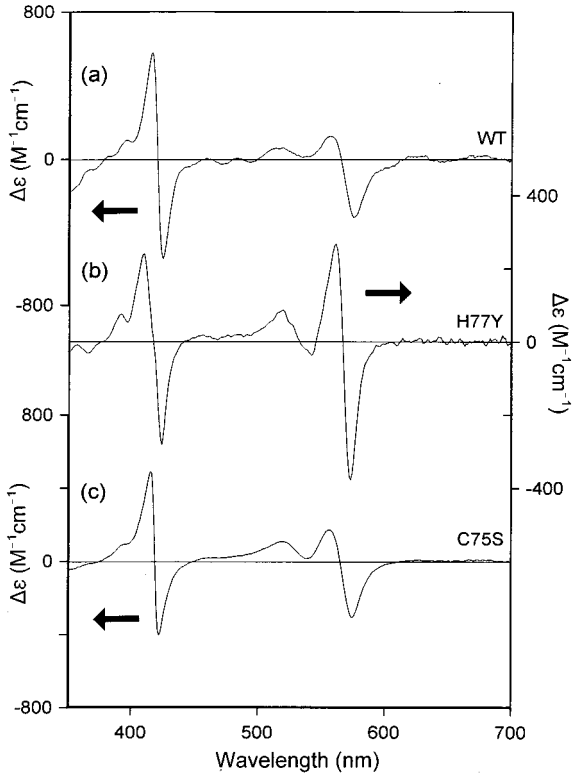

FIGURE 7: MCD spectra of dithionite-reduced CO-bound forms of WT, H77Y, and C75S CooA. (a) WT CooA at 78 K with a magnetic field of 6.0 T. (b) H77Y CooA at 86 K with a magnetic field of 4.5 T. (c) C75S CooA at 76 K with a magnetic field of 4.5 T. The samples were identical to those used in Figure 5.

signal-to-noise, were obtained at 4.2 K provided the samples were kept in the dark once frozen and the spectra were recorded with the minimum slit width (spectral bandwidth = 0.1 nm) and a faster scan rate. Even under these conditions, some photolysis occurred for WT CooA during data acquisition, indicating exquisite sensitivity to light-mediated Fe−CO bond cleavage at low temperatures. The MCD spectra of the low-spin Fe(II) CO adducts of WT and C75S CooA are identical within experimental error with *A*-terms centered at 420 and 565 nm in the Soret- and α-band regions, respectively. The spectra are very similar to the room-temperature MCD spectra of low-spin Fe(II) hemes with His/CO axial ligation, e.g., CO-bound myoglobin (*39*), as well as the reduced CO-bound forms of P420 (*27*), C420 (*32*), and H450 (*45*), and quite distinct from those of CO-bound forms of reduced P450 and iNOS which have Cys/CO axial ligation [*A*-terms centered at 447 and 561 nm in the Soret- and α-band regions, respectively (*46, 47*)]. The MCD spectrum of the low-spin Fe(II) CO adduct of the H77Y variant has analogous MCD bands at the same energies, but differs in terms of the relative intensities of the *A*-terms in the Soret- and α-band regions compared to WT and C75S. Such differences could result from a different ligand trans to CO or from changes in the polarity or hydrogen-bonding interactions in the CO-binding pocket. In light of the close similarity in the MCD spectra of the low-temperature photolysis products of these three samples, we favor the latter interpretation. Hence, in accord with the resonance Raman data of Spiro and co-workers (*17*), the VTMCD data indicate that CO binding to the low-spin Fe(II) heme of CooA occurs with displacement of His77 and retention of the yet-to-be-identified histidine or amine-type ligand.

CONCLUSIONS

The UV/visible/near-IR VTMCD studies reported herein have provided important new insights into the heme axial ligation, spin states, and CO-sensing mechanism of CooA. By investigating WT, H77Y, and C75S CooA, VTMCD has provided confirmatory evidence that Cys75 is one of the heme ligands in the oxidized protein and that it is replaced as an axial ligand by His77 on reduction (*13, 15*). The near-IR VTMCD and EPR evidence for a bis-histidine or histidine/amine ligated low-spin Fe(III) heme in the C75S variant leads to the conclusion that a histidine or amine-type ligand is trans to Cys75 in WT CooA. This suggests that His77 is capable of ligating the oxidized heme in CooA in the absence of Cys75. Moreover, UV−visible VTMCD studies indicate that this histidine or amine ligand remains ligated to the six-coordinate low-spin Fe(II) hemes in reduced and CO-bound forms of reduced CooA and to the five-coordinate high-spin Fe(II) heme formed by CO photolysis at low temperatures. Strong evidence that CO binding occurs with displacement

of His77 comes from the close similarity in the low-temperature MCD spectra of the five-coordinate high-spin Fe(II) CO photolysis products in the WT, H77Y, and C75S CooA. While the VTMCD studies reported herein do not address whether His77 is bound as histidine or histidinate, the results support the redox and CO-induced changes in heme ligation that have been proposed on the basis of resonance Raman studies (see Figure 4 of ref *17*), and identify the protein ligand X as histidine, lysine, arginine, or an N-terminal amine. Finally, the close correspondence of the UV−visible VTMCD (oxidized, reduced, and reduced plus CO) and EPR (oxidized) properties of CooA with those of P420 and C420 indicates that these inactive forms of P450 and chloroperoxidase are likely to have similar axial ligation and may undergo similar redox and CO-induced changes in axial ligation.

ACKNOWLEDGMENT

We thank Professor Judith N. Burstyn for critical reading of the manuscript and Robert Kerby for helpful discussions.

REFERENCES

1. Craven, P. A., and DeRubertis, F. R. (1983) *Biochim. Biophys. Acta 745*, 310−321.
2. Ignarro, L. J., Degnan, J. N., Baricos, W. H., Kadowitz, P. J., and Wolin, M. S. (1982) *Biochim. Biophys. Acta 718*, 49−59.
3. Yu, A. E., Hu, S. Z., Spiro, T. G., and Burstyn, J. N. (1994) *J. Am. Chem. Soc. 116*, 4117−4118.
4. Gilles-Gonzalez, M. A., Ditta, G. S., and Helinski, D. R. (1991) *Nature 350*, 170−172.
5. Gilles-Gonzalez, M. A., Gonzalez, G., and Perutz, M. P. (1995) *Biochemistry 34*, 232−236.
6. Rodgers, K. R., Kukatrodgers, G. S., and Barron, J. A. (1996) *Biochemistry 35*, 9539−9548.
7. Aono, S., Nakajima, H., Saito, K., and Okada, M. (1996) *Biochem. Biophys. Res. Commun. 228*, 752−756.
8. Shelver, D., Kerby, R. L., He, Y., and Roberts, G. P. (1997) *Proc. Natl. Acad. Sci. U.S.A. 94*, 11216−11220.
9. Shelver, D., Kerby, R. L., He, Y., and Roberts, G. P. (1995) *J. Bacteriol. 177*, 2157−2163.
10. Kerby, R. L., Hong, S. S., Ensign, S. A., Coppoc, L. J., Ludden, P. W., and Roberts, G. P. (1992) *J. Bacteriol. 174*, 5284−5294.
11. Kerby, R. L., Ludden, P. W., and Roberts, G. P. (1995) *J. Bacteriol. 177*, 2241−2244.
12. He, Y., Shelver, D., Kerby, R. L., and Roberts, G. P. (1996) *J. Biol. Chem. 271*, 120−123.
13. Shelver, D., Thorsteinsson, M. V., Kerby, R. L., Chung, S.-Y., Roberts, G. P., Reynolds, M. F., Parks, R. B., and Burstyn, J. N. (1999) *Biochemistry 38*, 2669−2678.
14. Reynolds, M. F., Shelver, D., Kerby, R. L., Parks, R. B., Roberts, G. P., and Burstyn, J. N. (1998) *J. Am. Chem. Soc. 120*, 9080−9081.
15. Aono, S., Ohkubo, K., Matsuo, T., and Nakajima, H. (1998) *J. Biol. Chem. 273*, 25757−25764.
16. Uchida, T., Ishikawa, H., Takahashi, S., Ishimori, K., Morishima, I., Ohkubo, K., Nakajima, H., and Aono, S. (1998) *J. Biol. Chem. 273*, 19988−19992.
17. Vogel, K. M., Shelver, D., Kerby, R. L., Thorsteinsson, M. V., Roberts, G. P., and Spiro, T. G. (1999) *Biochemistry 38*, 2679−2687.
18. Dawson, J. H., and Dooley, D. M. (1989) in *Iron Porphyrins, Part 3* (Lever, A. B. P., and Gray, H. B., Eds.) pp 1−135, VCH Publishers, New York.
19. Cheesman, M. R., Greenwood, C., and Thomson, A. J. (1991) *Adv. Inorg. Chem. 36*, 201−255.
20. Gadsby, P. M. A., and Thomson, A. (1990) *J. Am. Chem. Soc. 112*, 5003−5011.
21. Thomson, A. J., and Gadsby, P. M. A. (1990) *J. Chem. Soc., Dalton Trans.*, 1921−1928.
22. Johnson, M. K. (1988) in *Metal Clusters in Proteins* (Que, L., Jr., Ed.) *ACS Symp. Ser. 372*, 326−342.
23. Thomson, A. J., Cheeseman, M. R., and George, S. J. (1993) *Methods Enzymol. 226*, 199−232.
24. Aasa, R., and Vänngård, T. (1975) *J. Magn. Reson. 19*, 308−315.
25. McKnight, J., Cheesman, M. R., Thomson, A. J., Miles, J. S., and Munro, A. W. (1993) *Eur. J. Biochem. 213*, 683−687.
26. Lipscomb, D. J. (1980) *Biochemistry 19*, 3590−3599.
27. Martinis, S. A., Blanke, S. R., Hager, L. P., Sligar, S. G., Hoa, G. H. B., Rux, J. J., and Dawson, J. H. (1996) *Biochemistry 35*, 14530−14536.
28. Wuttke, D. S. (1994) Ph.D. Thesis, California Institute of Technology.
29. Omura, T., Sadano, H., Hasegawa, T., Yoshida, Y., and Kominami, S. (1984) *J. Biochem. 96*, 1491−1500.
30. Hollenberg, P. F., Hager, L. P., Blumberg, W. E., and Peisach, J. (1980) *J. Biol. Chem. 255*, 4801−4807.
31. Sono, M., Hager, L. P., and Dawson, J. H. (1991) *Biochim. Biophys. Acta 1078*, 351−359.
32. Blanke, S. R., Martinis, S. A., Sliger, S. G., Hager, L. P., Rux, J. J., and Dawson, J. H. (1996) *Biochemistry 35*, 14537−14543.
33. Poulos, T. L., and Raag, R. (1992) *FASEB. J. 6*, 674−679.
34. Crane, B. R., Arvai, A. S., Ghosh, D. K., Wu, C., Getzoff, E. D., Stuehr, D. J., and Tainer, J. A. (1998) *Science 279*, 2121−2126.
35. Finnegan, M. G., Knaff, D. B., Qin, H., Gray, K. A., Daldal, F., Yu, L., Yu, C.-A., Francisco, S. K.-S., and Johnson, M. K. (1996) *Biochim. Biophys. Acta 1274*, 9−20.
36. Lever, A. B. P., and Gray, H. B. (1983) in *Iron Porphyrins, Part 2*, pp 55−62, Addison-Wesley Publishing Co., Reading, MA.
37. Dawson, J. H., Andersson, L. A., and Sono, M. (1982) *J. Biol. Chem. 257*, 3606−3617.
38. Wells, A. V., Li, P., Champion, P. M., Martinis, S. A., and Sligar, S. G. (1992) *Biochemistry 31*, 4384−4393.
39. Svastits, E. W., and Dawson, J. H. (1986) *Inorg. Chim. Acta 123*, 83−86.
40. Vickery, L., Nozawa, T., and Sauer, K. (1976) *J. Am. Chem. Soc. 98*, 343−350.
41. Springall, J., Stillman, M. J., and Thomson, A. J. (1976) *Biochim. Biophys. Acta 453*, 494−501.
42. Brittian, T., Greenwood, C., Springall, J. P., and Thomson, A. J. (1982) *Biochim. Biophys. Acta 703*, 117−128.
43. Greschner, S., Sharonov, Y. A., and Jung, C. (1993) *FEBS Lett. 315*, 153−158.
44. Thomson, A. J., and Johnson, M. K. (1980) *Biochem. J. 191*, 411−420.
45. Svastits, E. W., Alberta, J. A., Kim, I., and Dawson, J. H. (1989) *Biochem. Biophys. Res. Commun. 165*, 1170−1176.
46. Dawson, J. H., Andersson, L. A., and Sono, M. (1983) *J. Biol. Chem. 258*, 13637−13645.
47. Sono, M., Stuehr, D. J., Ikeda-Saito, M., and Dawson, J. H. (1995) *J. Biol. Chem. 270*, 19943−19948.

BI991303C